



## Performance of free surface capturing methods in the wave absorption

Carolina Maria Nunes Bezerra<sup>1</sup>, Raquel Jahara Lobosco<sup>2</sup>, Jose Antonio F. Santiago<sup>1</sup>, Edmundo G. de A. Costa<sup>1</sup>

<sup>1</sup>Department of Civil Engineering, COPPE– UFRJ, Rio de Janeiro/RJ, Brazil

<sup>2</sup>Department of Mechanics Engineering, UFRJ, Macaé/RJ, Brasil

carolmnb@coc.ufrj.br, raquelobosco@macae.ufrj.br, santiago@coc.ufrj.br, edmundo\_costa@coc.ufrj.br

**Abstract.** Different numerical methodologies provided in the literature, associated to Computational Fluid Dynamics (CFD), are applied to generation and absorption of marine waves into a Numerical Wave Tank (NWT) model. However, when the user configures this problem in CFD, it is necessary to select the most appropriate numerical model to represent the physical phenomenon of wave motion. A standard framework for numerical modeling is the OpenFOAM software and its two-phase solvers as InterFoam and InterIsoFoam, which allow an adequate simulation for a wide range of marine hydrodynamic problems. A very common issue that appears in NWTs is the low capacity of absorption of the marine waves at the inlet and outlet into the numerical models. An efficient absorption of these waves is important to guarantee the open ocean conditions and to minimize the error associated with the numerical results. In order to mitigate the wave reflections, a numerical study of the convergence parameters applied to two-phase solvers was carried out and an analyse of the waves generation and absorption was performed. The present study allowed to evaluate the hydrodynamic interface treating methods available in OpenFOAM and foster a discussion of the already established methods.

**Keywords:** Interface capturing methods, OpenFOAM, Waves, Free surface flow

### 1 Introduction

The investigation of wave surface motion exists in many applications for the solution of problems that involve periodic and unsteady free surface of the biphasic flows. In the literature, some of the numerical methods cited to represents free surface motion are: interface tracking method [1], interface capturing methods [2], Marker-and-cell or MAC Scheme [3] and Volume-of-fluid or VOF scheme [4].

In the engineering field, specially about hydrodynamics of the waves, the correct knowledge of the wave characteristics is really important for the project of the ocean structures, such as generation, propagation, transformation along the motion and breaking near the coast. In the face of that challenge, the use of numerical models that provide a reliable results for a proper validation is required [5].

The CFD package OpenFOAM is the widely-used and is becoming increasingly popular. Its interFoam and interIsoFoam multiphase solvers have been utilized to simulate the wave motions by many authors in the literature, [? ]. However, depending the user sets for the CFD problem, the representation of the wave may not provide proper results. One barrier for the application of that solvers is the lack of suitable wavemaking and absorption capabilities [6]. This paper intended to approach the capabilities of interFoam and interIsoFoam solvers for propagation and absorption of a regular wave, in a bidimensional laminar flume. Both solvers have a default different settings for interface representation: MULES (interFoam) and isoAdvector (interIsoFoam), and this paper shows qualitatively its interference in the results.

### 2 Governing equations

The mass conservation (1) and momentum equations (2) are used for the numerical representation of free surface flow. The Eulerian approach was used to solve the Navier-Stokes Equations, and the flow is considered laminar and incompressible.

$$\frac{\partial U_i}{\partial x_i} = 0 \quad (1)$$

$$\frac{\partial(\rho U_i)}{\partial t} + \rho U_j \frac{\partial U_i}{\partial x_j} = -\frac{\partial p}{\partial x_i} + \rho g_i + \frac{\partial[\mu(\frac{\partial U_i}{\partial x_j} + \frac{\partial U_j}{\partial x_i})]}{\partial x_j} \quad (2)$$

where  $U$  is velocity,  $\rho$  is density,  $g$  is gravity acceleration,  $p$  is pressure, and  $\mu$  is dynamic viscosity.

### 3 Numerical model

In the present paper, three multiphase solvers were applied to represent a wave tank numerically. The solvers are based in the interface capturing method by using the Volume of Fluid method [4]. In the VOF method, the Equation (2) is solved for the two immiscible fluids simultaneously, where the fluids are tracked using the volume fraction scalar field,  $\alpha$ , which is 0 for air and 1 for water, any intermediate value is a mixture of the two fluids. The free surface is assumed to be at  $\alpha = 0.5$ . The scalar field  $\alpha$  is modelled by an advection term given by Equation (3).

$$\frac{\partial \alpha}{\partial t} + \nabla \cdot (U\alpha) = 0 \quad (3)$$

The properties density,  $\rho$  and viscosity,  $\mu$  are defined by the Equation (4) and (5) respectively.

$$\rho = \rho_{water}\alpha + \rho_{air}(1 - \alpha) \quad (4)$$

$$\mu = \mu_{water}\alpha + \mu_{air}(1 - \alpha) \quad (5)$$

The advection equation is purely convective. Therefore, high-order numerical methods are needed to minimize numerical diffusion. These numerical schemes are presented in the Subsections 3.1 and 3.2.

#### 3.1 The MULES solver

The MULES (Multidimensional Universal Limiter for Explicit Solution) is a numerical method in which the advection term of the Equation 3 is modified to compress the interface. Equation 6 represents an Integration of the advection equation with a temporal discretization scheme of the first term and a sum of the volume of all faces of the elements, in the second term.

$$\frac{\alpha_i^{n+1} - \alpha_i^n}{\Delta t} = -\frac{1}{|\Omega_i|} \sum_{f \in \partial\Omega_i} (F_u + \lambda_M F_c)^n \quad (6)$$

Where  $\Omega_i$ ,  $\partial\Omega_i$ , and  $\lambda_M$  are respectively the volume, the face of the volume, and a delimiter that indicates 1 for the surface and 0 for the region outside the interface. The terms  $F_u$  and  $F_c$  are the advective terms, described according to Equations 7 and 8.

$$F_u = \Phi_f \alpha_{f,upwind} \quad (7)$$

$$F_c = \Phi_f \alpha_f + \Phi_{rf} \alpha_{rf}(1 - \alpha)_{rf} - F_u \quad (8)$$

The subscript  $f$  indicates the amount evaluated on the face. *upwind* is the numerical scheme applied. The advective flow on the face is given by  $\Phi_f \alpha_f$  while  $\Phi_{rf} \alpha_{rf}(1 - \alpha)_{rf}$  represents the compressive flow. In Equation 6, the summation term represents the combination of the high-order scheme for advection and a compressive flow term, which allows for higher precision and decreased numerical diffusion in the interface, as well as the parameter of the stain aspect.

#### 3.2 The isoAdvect solver

The approach of the isoAdvect method is the usage of isosurface calculations to estimate the distribution of fluids inside the computational cells, [7]. The phase fraction is based on the time  $t$  from a function  $H(x, t)$ , as shown in Equation 9.

$$\alpha_i(t) = \frac{1}{V_i} \int_{\Omega_i} H(x, t) dV \quad (9)$$

The phase fraction  $\alpha_i$  can be obtained in the following time interval, by the Equation 10. The Equation 11 represents the total volume of fluid  $A$  transported through the face  $j$  during a time interval. The terms  $V_i$ ,  $\Omega_i$ ,  $B_i$ ,  $F_j$ ,  $s_{ij}$  and  $\tau$  are, respectively, the volume of cell  $i$ , the volume of each cell  $i$ , list of all faces, face  $j$  that belongs to cell  $i$ , term that guides the flow out of the volume, and the integration variable used in each time interval. Thus, the quantity that is estimated in the isoAdvector method is defined, through the fraction of the phase  $\alpha_i$ , velocity  $U_i$  and flow  $\Phi_j$  that crosses the face  $j$  in time  $t$ , according to Equation 12.

$$\alpha_i(t + \Delta t) = \alpha_i(t) - \frac{1}{V_i} \sum_{j \in B_i} s_{ij} \Delta V_j(t, \Delta t) \quad (10)$$

$$\Delta V_j(t, \Delta t) = \int_t^{t+\Delta t} \int_{F_j} H(x, \tau) U(x, \tau) dS d\tau \quad (11)$$

$$\Phi_j(t) = \int_{F_j} U(x, t) dS \quad (12)$$

## 4 The case of study

The test case corresponds to a regular wave propagation of a 2-D flume. The free surface position and velocity profiles are given by second order Stokes wave. The computational domain is shown in Figure 1 and corresponds to the length of  $3.79m$ , height of  $0.8m$  and constant water depth with  $0.4m$ . The domain is discretised with  $\Delta x = 0.01m$  and  $\Delta y = 0.005m$ , aspect ratio  $AR = \Delta x / \Delta y = 2$  and  $379 \times 160$  cells. For the simulation, the wave properties are: wave height  $H = 0.04m$ , wave period  $T = 2.0s$  and wave length  $\lambda = 3.79m$ . The time step is  $0.0001s$  and the total time of the simulation is  $180.0s$ .

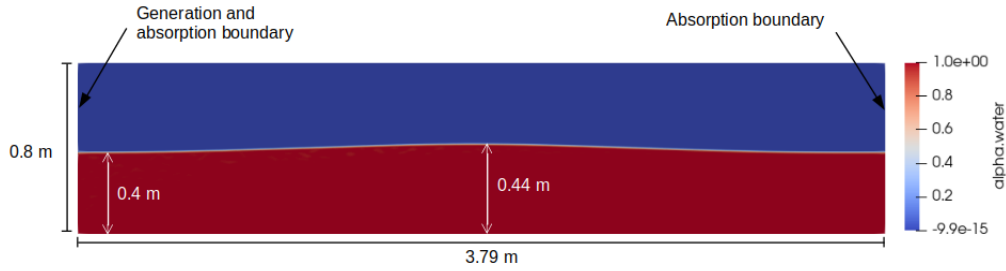


Figure 1. Case of study and dimensions of the computational domain.

For the second order Stokes wave [8], the free surface elevation and the velocity profiles are given by follow equations:

$$\eta = \frac{H}{2} \cos(kx - wt + \phi) + k \frac{H^2}{4} \frac{3 - \tanh^2(kh)}{4 \tanh^4(kh)} \cos(2(kx - wt + \phi)) \quad (13)$$

$$u = \frac{H}{2} \omega \cos(kx - wt + \phi) \frac{\cosh(kz)}{\sinh(kh)} + \frac{3H^2 \omega k}{16} \frac{\cosh(2kz)}{\sinh^4(kh)} \cos(2(kx - wt + \phi)) \quad (14)$$

$$v = \frac{H}{2} \omega \sin(kx - wt + \phi) \frac{\sinh(kz)}{\sinh(kh)} + \frac{3H^2 \omega k}{16} \frac{\sinh(2kz)}{\sinh^4(kh)} \sin(2(kx - wt + \phi)) \quad (15)$$

The case setup, at the OpenFOAM solver is showed by Tables 1 and 2. The numerical schemes are the same for both solvers. It is important to highlight that the results analysed in the present work has been proceed adjusting just the Courant numbers. Some of the other parameters that are relevant for the problem solution are the definition of *surfCellTol* and the *prgh* tolerance presents in the interIsoFoam solver. The *surfCellTol* tolerance must be larger than *prgh* tolerance by 1 – 2 orders of magnitude, since this avoid the air bubbles in the water phase.

Table 1. Basic setup of the wave study.

fvSchemes	Scheme
ddt	Euler
grad	Gauss linear
div(rhoPhi,U)	Gauss limitedLinearV 1
div(phi,alpha)	Gauss vanLeer
div(phirb,alpha)	Gauss linear
laplacian	Gauss linear corrected
interpolation	linear
snGrad	corrected

Table 2. fvSolution setup for the solvers.

fvSolution	interFoam
nAlphaCorr/cAlpha	1
nAlphaSubCycles	3
pcorr/prgh(solver, prec, tol)	PCG, DIC, 1e-6
prghFinal(solver, prec, tol)	GAMG, DIC, 1e-7
U/UFinal(solver, prec, tol)	PBiCG, DILU, 1e-6
fvSolution	interIsoFoam
isoFaceTol	1e-10
surfCellTol	1e-5
nAlphaBounds	3
snapTol	1e-12
clip	True
reconstructionScheme	isoAlpha
pcorr/prgh/prghFinal(solver, prec, tol)	PCG, DIC, 1e-6
U(solver, smoother, tol)	smoothSolver, symGaussSeidel, 1e-06

#### 4.1 Free surface flow

In this section, the results of interFoam and interIsoFoam solvers will be compared with the free surface elevation given by 2nd Stokes theory. The free surface numerical profile corresponds to elevation of the crest in the time of  $35.25T$ . The Figures 2(a) to 3(b) provides the qualitative information of the crest elevation and the respective error with relation to 2nd order Stokes solution for three Courant ( $Co$ ) numbers. In the multiphase solver, there are two  $Co$  numbers that the user must define: the  $maxCo$ , that means the maximum  $Co$  in the cells, and the  $maxAlphaCo$ , that means the maximum  $Co$  in the interface cells. Three tests were performed with different combinations of  $Co$  numbers for each solver.

For the interFoam solution, the  $maxCo = 0.15$  and  $maxAlphaCo = 0.25$  (Figure 2(a)) is noticeable the elevation of crest near the exact solution, but presenting larger errors in the other positions. The  $Co$  number showed a wiggled interface, leading to an inappropriate advection. The interFoam provided minor error results with  $maxCo = 0.15$  and  $maxAlphaCo = 0.20$ . In this case, it is important highlighting the time interval is controlled more by the velocities near the interface. For the interIsoFoam solution, the results maintained nearest the exact solution (Figure 3(a)). The low  $Co$  numbers,  $maxCo = 0.02$  and  $maxAlphaCo = 0.01$ , provided a minor error in comparison with interFoam, with a good representation of the interface.

For the next results, it was considered the  $Co$  numbers that presented the minor error for each solver, i.e, for interFoam,  $maxCo = 0.15$  and  $maxAlphaCo = 0.20$ , for interIsoFoam,  $maxCo = 0.02$  and  $maxAlphaCo = 0.01$ .

The Figure 4 shows the distribution of the vertical velocity beneath the crest with relation to the best result of  $Co$  number for each simulation, provided by the previous results. It is verified there is a slight perturbation in the interFoam solution, what is not observed in the velocity distribution provided by interIsoFoam.

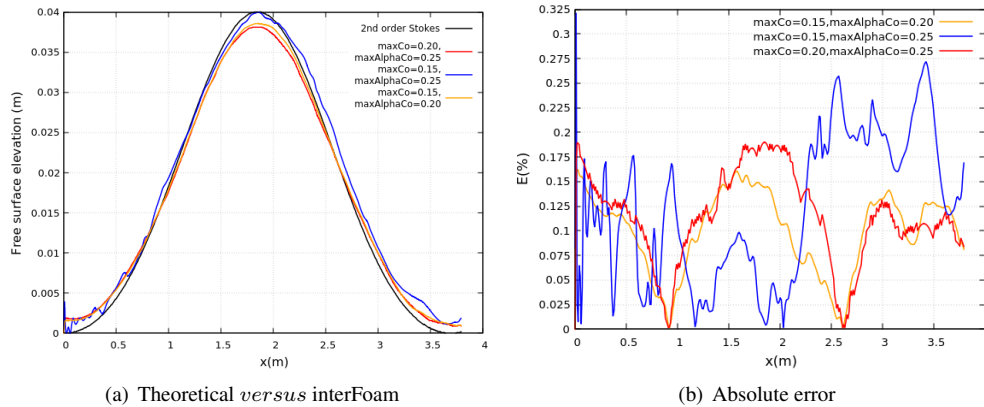


Figure 2. Free surface elevation for different Co numbers (interFoam).

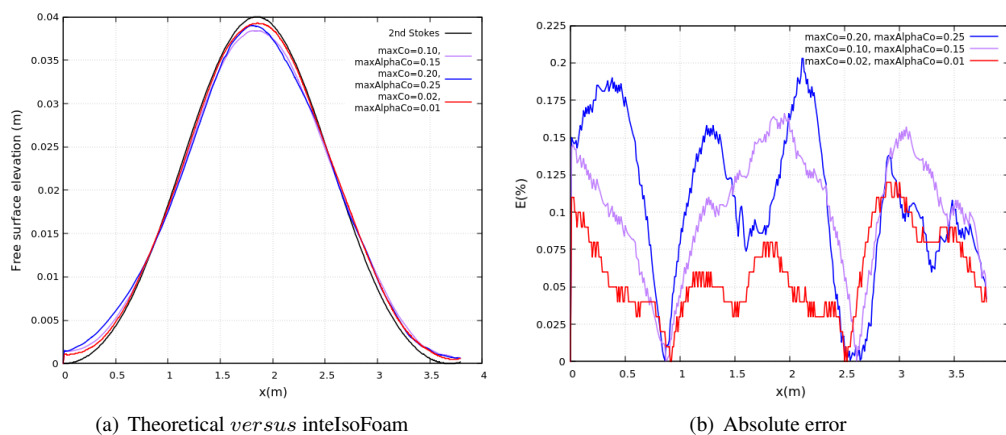


Figure 3. Free surface elevation for different Co numbers (interIsoFoam).

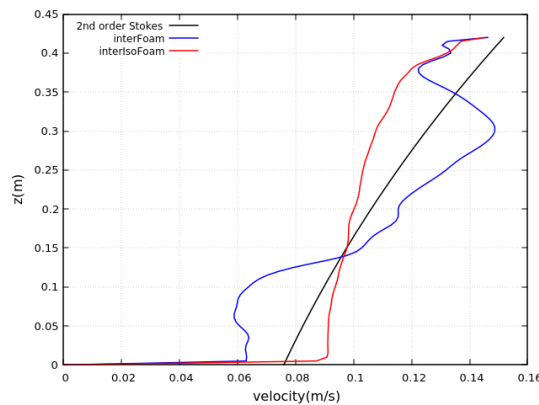


Figure 4. Velocity distribution beneath the crest at  $t=35.25T$

#### 4.2 Wave absorption effect

In Figures 5(a) to 5(d) the vertical velocity profile near the outlet, at  $x = 3.72m$  are presented. The results show that, the velocity field is modified by a wave reflection with a wave propagation. It is possible to note that the interIsoFoam showed good wave absorption capacity. The behaviour of the wave slight increases the velocity near the interface, and crossing to the air region, the velocity decreases approximately to zero values. The results provided by interFoam showed a strong effect of the wave reflection, specially noted in the water region.

In Figure 6 the velocity field near the outlet boundary condition (positions  $x = 3.72m$  to  $x = 3.79m$ ) is shown for both simulations with interFoam and interIsoFoam. Here it is quite clear that interIsoFoam, with the

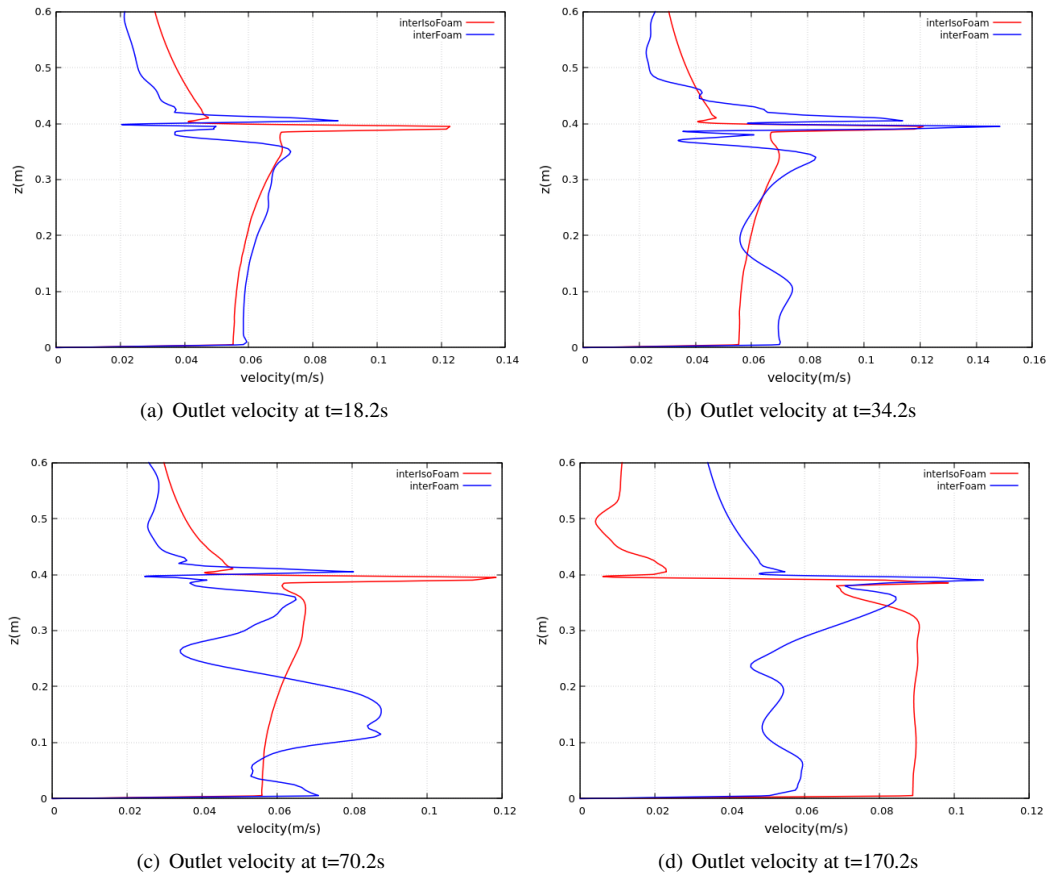


Figure 5. Velocity absorption profile.

current settings, improve the wave absorption. Beneath of the free surface, the interFoam presented dissipation in the velocity field and low wave absorption capacity beneath the free surface. However, it is possible to note for both solvers that the mass transfer water/air still effect the results, since Figure 6 shown a low velocity in the air phase.

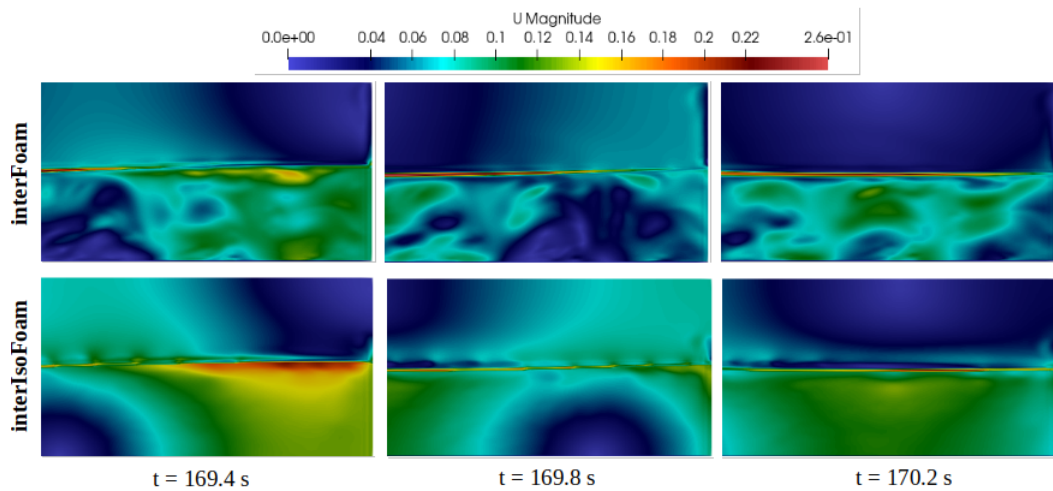


Figure 6. Velocity profile in the outlet absorption region.

## 5 Conclusions

In this paper the qualitative analyses of the interFoam and interIsoFoam for a regular progressive wave has been presented. The fluid flow has been considered incompressible, laminar and with no viscosity. The results of the free surface profile for three different Courant numbers combination for cells and interface cells has been shown sensivity in the results.

The adjust of Co numbers depends of the mesh resolution and time step for the solution. As both of them are small, the Co number is small as well, insured that the fluid moves into the face neighbours cells during the time step. In the isoAdvector algorithm, the interface in a cell is treated as approximately planar and moving with constant velocity during the time step. Hence, it is necessary a small Co number for the precision not be lost and the advection at interface be done correctly.

The results of the wave absorption have showed the influence of the wave reflection at near the outlet. For interIsoFoam, the good absorption may be attributed to the small Co number that controlled the field velocity in the interface region, presented more accurated results for free surface (Figure 4.1) and velocity (Figures 5(a)-5(d) and 6). On the other hand, the interFoam solver showed be more dissipative than interIsoFoam, according to Figure 6 and perturbations in the velocity profiles for interval  $t > 18.2s$  highlighting divergence in results.

**Acknowledgements.** The authors are grateful for the support of the following funding agencies: CAPES (Coordination for the Improvement of Higher Education Personnel) and FAPERJ (Carlos Chagas Foundation for Research Support of the State of Rio de Janeiro).

**Authorship statement.** The authors hereby confirm that they are the sole liable persons responsible for the authorship of this work, and that all material that has been herein included as part of the present paper is either the property (and authorship) of the authors, or has the permission of the owners to be included here.

## References

- [1] J. M. Hyman. Numerical methods for tracking interfaces. *Physica D: Nonlinear Phenomena*, vol. 12, n. 1, pp. 396–407, 1984.
- [2] S. Mirjalili, S. Jain, and M. Dodd. Interface-capturing methods for two-phase flows: An overview and recent developments. *Center for Turbulence Research - Annual research brief*, pp. 117–135, 2017.
- [3] F. H. Harlow and J. E. Welch. Numerical Calculation of Time-Dependent Viscous Incompressible Flow of Fluid with Free Surface. *Physics of Fluids*, vol. 8, n. 12, pp. 2182–2189, 1965.
- [4] C. Hirt and B. Nichols. Volume of fluid (vof) method for the dynamics of free boundaries. *Journal of Computational Physics*, vol. 39, n. 1, pp. 201–225, 1981.
- [5] J. Conde. Comparison of different methods for generation and absorption of water waves, 2019.
- [6] P. Schmitt, C. Windt, J. Davidson, J. Ringwood, and T. Whittaker. Beyond vof: alternative openfoam solvers for numerical wave tanks. *Journal of Ocean Engineering and Marine Energy*, 2020.
- [7] H. B. J. Roenby and H. Jasak. A computational method for sharp interface advection. *The Royal Society Open Science*, 2016.
- [8] P. Lin. *Numerical Modeling of Water Waves*. CRC Press, 2004.